Title:

Kinobead/LC-MS phosphokinome profiling enables rapid analyses of kinase-dependent cell signaling networks

Authors:

Martin Golkowski,[1]* Venkata Narayana Vidadala,[2] Ho-Tak Lau,[1] Anna Shoemaker,[1] Masami Shimizu-Albergine,[3] Joseph Beavo,[1] Dustin J. Maly,[2] and Shao-En Ong.[1]*

[1]Department of Pharmacology, University of Washington, Seattle, WA 98195, USA

[2]Department of Chemistry, University of Washington, Seattle, WA 98195, USA

[3]University of Washington Medicine Diabetes Institute, University of Washington, Seattle, WA 98109, USA

*Correspondence: shaoen@u.washington.edu (S-E.O.), golkom@uw.edu (M.G.)

Abstract:

Kinase-catalyzed protein phosphorylation is fundamental to eukaryotic signal transduction, regulating most cellular processes. Kinases are frequently dysregulated in cancer, inflammation and degenerative diseases, and because they can be inhibited with small molecules, they became important drug targets. Accordingly, analytical approaches that determine kinase activation states are critically important to understand kinase-dependent signal transduction, and to identify novel drug targets and predictive biomarkers. Multiplexed inhibitor beads (MIBs or kinobeads) efficiently enrich kinases from cell lysates for LC-MS analysis. When combined with phosphopeptide enrichment, kinobead/LC-MS can also quantify the phosphorylation state of kinases, which determines their activation state. However, an efficient kinobead/LC-MS kinase phospho-profiling protocol that allows routine analyses of cell lines and tissues has not yet been developed. Here, we present a facile workflow that quantifies the global phosphorylation state of kinases with unprecedented sensitivity. We also found that our kinobead/LC-MS protocol can measure changes in kinase complex composition and show how these changes can indicate kinase activity. We demonstrate the utility of our approach in specifying kinase signaling pathways that control the acute steroidogenic response in Leydig cells; this analysis establishes the first comprehensive framework for the post-translational control of steroid biosynthesis.

Keywords:

Mass spectrometry, chemoproteomics, kinobeads, protein kinase, steroidogenesis.

Introduction:

Protein kinases are central regulators of eukaryotic cell signaling pathways that control most cellular processes.[1] Kinase-dependent signaling pathways are frequently dysregulated in disease, for instance cancer, inflammatory, infectious and degenerative diseases, and because of that kinases have become major drug targets.[2-3] Approaches that measure the activity of kinases are critically important to study the physiological function of kinase-dependent signaling pathways, and their dysregulation in disease. Signaling crosstalk between different kinase-dependent pathways is fundamental to cellular information processing and causes the formation of highly dynamic, complex and interconnected signaling networks.[4-5] Because of this network structure, kinases are best studied at the systems-level and methods that allow highly multiplexed analyses of kinase regulation are highly desirable.[6]

Protein kinases activity depends on post-translational modifications (PTMs), most importantly phosphorylation.[7-8] Global mass spectrometry (MS)-based proteomics allows system-wide and unbiased measurements of PTMs, and should be well suited to analyze the activity of protein kinases. However, unlike many of their substrates, kinases are of low abundance in cells and typically underrepresented in global phosphoproteomics datasets.[9] To increase the analytical coverage of kinases, multiplexed inhibitor beads (MIBs or kinobeads) were introduced; these affinity matrices enrich most cellular kinases for downstream LC-MS analyses of protein expression and phosphorylation.[9-10] Although kinobead/LC-MS has been shown to be a powerful tool to analyze kinase phosphorylation, the approach has not been adopted for routine profiling of cell lines and tissues. We believe that this is due to the large sample requirements for single experiments, which precludes its use in high-throughput analyses or in limited amounts of tissue.[9, 11-14] We present here a facile workflow for comprehensive kinobead/LC-MS kinome profiling of cell or tissue lysates. We optimized sample preparation steps prior to LC-MS analysis, which greatly improved the sensitivity of the approach. These improvements now allow the analysis of the kinome's phosphorylation state, i.e. the phosphokinome, to a depth of ~800-1200 phosphosites from ~1 mg of protein sample in single LC-MS runs. Importantly, we also show that our kinobead/LC-MS platform can quantify changes in the composition of kinase complexes, and we demonstrate how these changes can be exploited to infer the activation state of kinases.

We utilized our kinobead/LC-MS kinome profiling protocol to quantify dynamic changes in the phosphokinome triggered by lutropin-choriogonadotropic hormone receptor (LHCGR) activation[15]. The LHCGR is a Gαs-coupled GPCR that controls the biosynthesis of steroid

hormones essential for the development and maintenance of gender-specific phenotypes.[16] Steroidogenesis is a highly complex process: to rapidly synthesize steroids following hormone stimulation, steroidogenic cells need to coordinate cholesterol uptake, it's mobilization from internal stores, transport and metabolism as well as the transcription of key steroidogenic proteins.[16] To understand how these processes are controlled by PTMs, our group previously conducted a global phosphoproteomics study in steroidogenic Leydig cells.[17] This study suggested that in addition to PKA and ERK1/2 a host of other kinases exert post-translational control of the acute steroidogenic response.[17-18] However, the identity of these kinases remained elusive. Furthermore, our previous study used cAMP phosphodiesterase (PDE) inhibitors to trigger the acute steroidogenic response, leaving the question how this process is controlled by native LHCGR signaling. We show here that LHCGR signaling in Leydig cells affects the phosphorylation and activation state of 106 protein kinases within minutes of luteinizing hormone (LH) stimulation. Many of these kinases regulate endocytosis, vesicle transport and cytoskeleton dynamics, all processes that are associated with cellular cholesterol uptake and transport.[19-20] Therefore, we greatly expand our knowledge of the post-translational control of steroid biosynthesis, and our dataset will serve as a rich resource for functional studies of steroidogenic cell signaling.

Experimental Procedures:

Cell culture, treatment and harvest

MA10 mouse Leydig tumor cells (Cat #CRL-3050, ATCC, Manassas, VA) and adherent HeLa cells (Cat #CCL-2, ATCC) were cultured in the ATCC-recommended medium supplemented with 10% FBS (for HeLa cells, Seradigm, VWR Life Science, Radnor, PA) or 15% horse serum (HS, for MA10 cells, Gibco, Thermo Fisher Scientific, Waltham, MA) and 100x penicillin-streptomycin-glutamine (Thermo Fisher Scientific). Before treatment with human recombinant LH (50 ng/mL, R&D Systems, Minneapolis, MN) or human recombinant EGF (50 ng/mL, R&D Systems) cells were serum starved in the corresponding FBS/HS-free medium for 18 hrs. Control treatment was vehicle (H_2O). For SILAC-labeling, MA10 cells were cultured in custom RPMI medium supplemented with 15% dialyzed fetal bovine serum (dFBS), 100x penicillin-streptomycin-glutamine, 20 µg/ml proline and the corresponding isotope labelled Lysine (Lys, 0.11 mM) and Arginine (Arg, 0.57 mM, light label = Lys0/Arg0, medium label = Lys4/Arg6, heavy label = Lys8/Arg10, all SILAC amino acids were from Cambridge Isotope Labs, Andover, MA). Cells were split every 2-3 days and grown for 7 cell doublings to achieve complete incorporation of isotope-labeled Lys/Arg. Before treatment with LH, cells were serum

starved with dFBS-free SILAC medium and treated as described above. For harvest, cells were washed twice with ice cold PBS and modified RIPA buffer (50 mM Tris, 150 mM NaCl, 0.25% Na-deoxycholate, 1% NP-40, 1 mM EDTA and 10 mM NaF, pH 7.8) supplemented with HALT protease inhibitor cocktail (100x, Thermo Fisher Scientific) and phosphatase inhibitor cocktail II and III (100x, Sigma-Aldrich, St Louis, MO) was added (100 µL for 6-well plates, 350 µL for 10 cm dishes). Cells were collected with a cell scraper, lysates vortexed intermittently at max. speed 5-times and clarified by centrifugation (20 min at 21,000 xg and 4°C). Protein content of lysates was determined using the Pierce 660 nm assay reagent (Thermo Fisher Scientific).

Western Blotting

Cell lysates in modified RIPA buffer were mixed with 4x NuPAGE LDS Sample Buffer (Thermo Fisher Scientific) and DTT was added to a final concentration of 50 mM. Samples were heated to 95°C for 5 min, proteins separated on Bolt 4-12% Bis-Tris Plus Gels (Thermo Fisher Scientific) and electro-transferred onto nitrocellulose membranes using standard procedures. Membranes were blocked with 5% non-fat dry milk powder in TBS containing 1% Tween 20 (TBST), incubated with primary antibodies overnight (1:2000 dilution in milk-TBST), and visualized with an anti-rabbit IgG, HRP-linked antibody (Cat #7074, Cell signaling Technology, Danvers, MA). Primary antibodies (all from Cell Signaling Technology) used were anti-phospho-p44/42 MAPK (Erk1/2) (Thr202/Tyr204) (Cat #4370), Phospho-PKA Substrate (RRXS*/T*) (100G7E) Rabbit mAb (Cat #9624) and p44/42 MAPK (Erk1/2) (137F5) Rabbit mAb (Cat #4695).

Preparation of optimized kinobead mixture

The seven kinobead affinity reagents used were synthesized in-house as described previously.[21-22] For optimal coverage of the human kinome an optimized mixture of the seven kinobead reagents was prepared as follows: 1 ml of reagent #1, 0.5 ml of reagents #2, #3 and #7, respectively, and 0.25 ml of reagents #4, #5 and #6, respectively, to give 3.25 ml of the complete kinobead mixture. All reagents were a 50% slurry in 20% aq. ethanol.

Kinase affinity enrichment and on-bead digestion

For each experiment, three micro tubes containing 35 µL of a 50% slurry of the in-house-made, optimized kinobead mixture in 20% aq. ethanol were prepared for each pulldown experiment. The beads were washed twice with 300 µL modified RIPA buffer. 1 mg of protein extract in modified RIPA buffer (see ‘Cell culture, treatment and harvest’ above) were added to

the first tube. The mixture was incubated on a tube rotator for 1h at 4°C and then the beads were spun down rapidly at 2000 rpm on a benchtop centrifuge (5s). The supernatant was pipetted into the next tube with kinobeads for the second round of affinity enrichment. The procedure was repeated once more for a total of three rounds of affinity enrichment. After removal of the supernatant, the beads were rapidly washed twice with 300 µL of ice-cold modified RIPA buffer and three times with 300 µL ice-cold tris-buffered saline (TBS, 50 mM tris, 150 mM NaCl, pH 7.8) to remove detergents. 100 µL of the denaturing buffer (20% trifluoroethanol (TFE),[23] 25 mM Tris containing 5 mM tris(2-carboxyethyl)phosphine hydrochloride (TCEP*HCl) and 10 mM chloroacetamide (CAM), pH 7.8), were added and the slurry vortexed at low speed briefly. At this stage, kinobeads from the three tubes were combined and heated at 95°C for 5 min. The mixture was diluted 2-fold with 25 mM triethylamine bicarbonate (TEAB), the pH adjusted to 8-9 by addition of 1 N aq. NaOH; 5 µg MS-grade lysyl endopeptidase Lys-C (Wako, Richmond, VA) were added and the mixture agitated on a thermomixer at 1400 rpm at 37°C for 2 h. Then 5 µg MS-grade trypsin (Thermo Fisher Scientific) were added, and the mixture agitated on a thermomixer at 1400 rpm at 37°C overnight. 600 µL of 1% formic acid were added and the mixture acidified by addition of an additional 6 µl of formic acid to yield 1.2 ml peptide solution in total. An aliquot of 120 µl (10%) of the peptide solution was desalted using StageTips[24] and analyzed by LC-MS/MS for protein quantification. The remaining peptide solution (90%) was dried under vacuum at RT on a SpeedVac. 300 µL of 70% aq. ACN + 0.1 % TFA was added to each tube, the mixture vortexed, and sonicated in a bath sonicator until dried peptide residue was dissolved. In case the dried residue could not be fully resuspended, additional 0.1% aq. TFA can be added in 10 µl increments until dissolved. The solution was subjected to IMAC phosphopeptide enrichment protocol (see 'IMAC phosphopeptide enrichment' below).

Preparation of peptides for global phosphoproteomics analyses

Cells were rinsed twice with ice cold PBS and harvested in 350 µL (10 cm dish) of 6 M aq. guanidine hydrochloride (Gdn*HCl) containing 100 mM Tris, 5 mM TCEP*HCl and 10 mM CAM, pH 8.5, using a cell scraper. Cell lysates were vortexed briefly and then heated to 95°C for 5 min.[25] Samples were sonicated in a Qsonica cup sonicator (Newton, CT) at 100 W for 10 min (30 seconds on, 30 seconds off) on ice. Protein content was measured using the Pierce 660 nm assay reagent (Thermo Fisher Scientific). Aliquots of 300 µg of protein were diluted 2-fold with 100 mM triethylammonium bicarbonate (TEAB) pH = 8.5 and adjusted to pH 8-9 with 1 N aq. NaOH. 3 µg of MS-grade lysyl endopeptidase Lys-C (Wako) were added (1:100 ratio) and

the mixture agitated on a thermomixer at 1400 rpm at 37°C for 2 h. The mixture was diluted another 2-fold with 100 mM TEAB pH 8.5 and 3 µg of MS-grade trypsin (Thermo Fisher Scientific) was added. The mixture was agitated on a thermomixer at 1400 rpm at 37°C for overnight, acidified with formic acid (1% final), and cleared by centrifugation for 10 min at RT and 14,000 xg. Peptides were extracted from the supernatant using Oasis HLB 1cc (10 mg) extraction cartridges (Waters, Milford, MA). Cartridges were activated by passing through 200 µl of methanol followed by 200 µl 80% aq. ACN containing 0.1% TFA, equilibrated with 400 µl 1% aq. formic acid. Peptides were loaded and then washed with 400 µl 1% aq. formic acid. Peptides were eluted with 300 µl 80% aq. ACN containing 0.1% TFA and directly subjected to IMAC phosphopeptide enrichment (see 'IMAC phosphopeptide enrichment' below).

IMAC phosphopeptide enrichment

IMAC phosphopeptide enrichment was performed according to the published protocol with the following modifications.[26] 20 µL of a 50% IMAC bead slurry composed of 1/3 commercial PHOS-select iron affinity gel (Sigma-Aldrich), 1/3 in-house made Fe^{3+}-NTA Superflow agarose and 1/3 in-house made Ga^{3+}-NTA Superflow agarose were used for phosphopeptide enrichment.[27] The IMAC slurry was washed three times with 10 bed volumes of 80% aq. ACN containing 0.1% TFA. Phosphopeptides were desalted using C18 StageTips according to the published protocol with the following minor modifications for phosphopeptides.[24] After activation with 50 µL methanol and 50 µL 80% aq. ACN containing 0.1% TFA the StageTips were equilibrated with 50 µL 1% aq. formic acid. Then the peptides that were reconstituted in 50 µl 1% aq. formic acid were loaded and washed with 50 µl 1% aq. formic acid.

LC-MS/MS analyses

Peptide samples were separated on a Thermo-Dionex RSLCNano UHPLC instrument (Sunnyvale, CA) using 20 cm fused silica capillary columns (100 µm ID) packed with 3 µm 120 Å reversed phase C18 beads (Dr. Maisch, Ammerbuch, DE). For whole peptide samples the LC gradient was 120 min long with 10−35% B at 300 nL/min. For phosphopeptide samples the LC gradient was 120 min long with 3−30% B at 300 nL/min. LC solvent A was 0.1% aq. acetic acid and LC solvent B was 0.1% acetic acid, 99.9% acetonitrile. MS data was collected with a Thermo Orbitrap Elite spectrometer. Data-dependent analysis was applied using Top15 selection with CID fragmentation. Raw files were analyzed by MaxQuant/Andromeda version 1.5.2.8 (http://www.maxquant.org) using protein, peptide and site FDRs of 0.01 and a score

minimum of 40 for modified peptides, 0 for unmodified peptides; delta score minimum of 17 for modified peptides, 0 for unmodified peptides. MS/MS spectra were searched against the UniProt human or mouse database (updated July 22nd, 2015). MaxQuant search parameters: Variable modifications included Oxidation (M). Carbamidomethyl (C) was a fixed modification. Max. labeled amino acids was 3, max. missed cleavages was 2, enzyme was Trypsin/P, max charge was 7, multiplicity was either 1, 2 or 3, SILAC labels were Arg0/Lys0 (light), Arg6/Lys4 (medium), Arg10/Lys8 (heavy). The MaxQuant Re-Quantification feature was enabled. The initial search tolerance for FTMS scans was 20 ppm and 0.5 Da for ITMS MS/MS scans. The MS raw files were uploaded to the MassIVE proteomics repository (https://massive.ucsd.edu) under the accession number MSV000084499.

MaxQuant data processing

MaxQuant output files were processed using the Perseus software package v1.5.6.0.[28] Human and mouse gene ontology (GO) terms (GOBP, GOCC and GOMF) were loaded from the 'Perseus Annotations' file downloaded on 01.08.2017. For LFQ experiments, expression columns (protein and phosphopeptide intensities) were log2 transformed and normalized by subtracting the median log2 expression value from each expression value of the corresponding data column. Data imputation was performed using a modeled distribution of MS intensity values downshifted by 1.8 and having a width of 0.2. For statistical testing of significant differences in protein and phosphopeptide abundance, a two-sample Student's T-test with Benjamini-Hochberg (BH) correction for multiple hypothesis testing was applied (FDR = 0.05). Where no data imputation was used, proteins that were quantified reliably only in one experimental condition but not in the other condition were highlighted and considered as regulated too (see 'Table S1').

Secondary data analysis

SILAC phosphokinome time course data was clustered using the Mfuzz package in R allowing 6 clusters and using a fuzzification factor of 2.[29] GOBP-term enrichment analysis was performed with STRING 11.0[30] using MaxQuant gene names of all proteins that significantly change in phosphorylation or expression in response to 15 min LH treatment (global phosphoproteomics and kinobead/LC-MS data) to determine LH-regulated pathways. The same analysis was repeated using all unchanged proteins to identify enrichment biases caused by quantification of specific subsets of the entire proteome. To determine the biological function and the kinase-substrate relationship of a given phosphorylation site the PhosphoSite Plus

datasets ‘Regulatory_Sites’ and ‘Kinase_Substrate_Dataset’ were searched against a short identifier containing the gene name and the 5 amino acid sequence centered on the phosphorylated residue. Human, mouse and rat phosphorylation sites were all considered to assess the biological and biochemical consequences of phosphorylation. The datasets were downloaded from the PhosphoSite Plus webpage on the 13th of March, 2017 (https://www.phosphosite.org)[31]. Protein kinase interactors were determined using the BioGRID database only considering protein-protein interactions for which two independent lines of evidence exist[32]. To that end, the ‘BIOGRID-MV-Physical-3.5.165.tab2’ file was downloaded on October 6th, 2018 and mined for protein kinase interactions through matching against the gene name in the MaxQuant output files.

Statistical analyses

All significant differences in protein and phosphopeptide abundance were determined using a two sample T-Test with BH correction (see ‘MaxQuant data processing’ above). All LFQ cell line experiments, i.e. hormone treatments of MA10 and HeLa cells were conducted in 4-6 biological replicates as indicated in Table S1. The SILAC time course experiment in MA10 cells was performed in 3 biological replicates.

Results:

A sensitive and streamlined protocol for deep phosphokinome profiling

Previous protocols for kinobead/LC-MS profiling of kinase phosphorylation required relatively large amounts of cellular protein (~100-400 mg) and kinobeads (~1.5-2.5 mL).[9, 12-14] These requirements discouraged the application of phosphokinome profiling in *in vitro* and *in vivo* model systems and made it impractical in clinical tissue samples. To reduce the sample requirements of kinobead/LC-MS profiling, we sought to increase analytical sensitivity of the approach by reducing sample losses arising from processing steps such as SDS-PAGE protein separation and peptide desalting before LC-MS analyses.[33]

We showed previously that SDS-gel separation and in-gel digestion of proteins can be replaced with an on-bead purification and digestion step to increase the analytical sensitivity of kinobead/LC-MS by up to 10-fold (Figure 1a).[21-22] However, peptide mixtures that result from on-bead digestion still contain high concentrations of buffer components such as urea or guanidine that are incompatible with immobilized metal affinity chromatography (IMAC) phosphopeptide enrichment.[26] To eliminate these buffer components, we incorporated the volatile denaturing

agent trifluoroethanol (TFE) into our workflow;[23] this allows IMAC enrichment of phosphorylated peptides from crude digestion mixtures without prior peptide desalting on C18 reversed-phase cartridges (Figure 1a). To test the analytical sensitivity of our TFE/on-bead preparation protocol, we employed our in-house developed kinobeads[34] to enrich kinases from untreated HeLa cell lysate using varying amounts of affinity beads (37.5-150 µL) and protein (0.5-5 mg, Figure 1b). After on-bead digestion, 10% of each peptide sample was analyzed in single LC-MS runs on an Orbitrap Elite MS instrument to quantify the protein expression of kinases and co-enriched non-kinase proteins. The remaining 90% of each peptide sample was subjected to IMAC phosphopeptide enrichment and then analyzed by LC-MS (Figure 1a). Our results show that the number of quantified protein kinases remained unchanged with varying amounts of affinity beads and lysate; this demonstrates the high sensitivity of kinase protein quantification achieved by our kinobead/LC-MS protocol. More importantly, when we reduced the amount of protein sample from 5 mg to 1 mg the number of quantified kinase and non-kinase phosphopeptides remained stable at ~750 and ~1400 peptides per LC-MS run (Figure 1b). Further reducing the protein sample from 1 mg to 0.5 mg lowered the number of quantified phosphopeptides by only 20%. The same trend was observed when we lowered the amount of kinobead affinity matrix from 150 µL to 37.5 µL using 1 mg of protein sample (Figure 1C). These results demonstrate that 1 mg of protein and 100 µL of kinobeads are enough to achieve deep coverage of the phosphokinome.

Kinobead/LC-MS analysis of EGF-dependent phosphokinome changes

We have established a highly sensitive kinobead/LC-MS workflow and wished to demonstrate next that our approach can accurately quantify system-wide changes in the phosphorylation and activation state of kinases.[13] As our model signaling system, we chose activation of the epidermal growth factor receptor (EGFR) in HeLa cells. This is a well-defined system and activation of the EGFR itself and known downstream kinases such as ERK1/2 and RSK-family kinases serve as positive controls for the accuracy of our kinobead/LC-MS analysis.[35-36]

We used label free quantification (LFQ) and kinobead/LC-MS to analyze untreated control and EGF-stimulated HeLa cells (50 ng/mL EGF for 15 min, 6 biological replicates/condition). This analysis quantified 1252 phosphosites on 196 protein kinases and 3771 phosphosites on 1217 co-enriched non-kinase proteins (Table S1), confirming that our workflow achieves deep coverage of the phosphokinome and the phosphorylation of kinase-interacting proteins. Because determining the activation state of kinases was an important goal

of our kinobead/LC-MS analyses we searched the Phosphosite Plus database[31] for phosphorylation sites with known functional roles in kinase signaling. This revealed that we quantified 160 sites on 84 kinases that directly indicate their activation state (Table S1). In addition, we quantified 485 sites on kinases and non-kinase proteins for which the kinase-substrate relationship is known; we used these sites as indirect activity reporters for 112 of the 226 kinases that we detected in HeLa cells. Combining these direct and indirect phospho-evidence allowed us to determine the activation state of 131 kinases, or 58% of the kinome detected in HeLa cells, demonstrating the utility of kinobead/LC-MS for highly multiplexed analyses of kinase activation.

To identify EGF-dependent changes in protein phosphorylation, we calculated mean LFQ-MS phosphopeptide intensities ratios (hereafter referred to as 'LFQ-MS ratio') and applied T-test statistics (Benjamini-Hochberg (BH) correction, FDR = 0.05). This revealed that 261 phosphosites on 120 kinases change in abundance within 15 min of EGF stimulation, meaning that half of the detected HeLa cell kinome is affected by early EGFR signaling (Table S1). Gratifyingly, among EGF-sensitive kinase phosphosites we identified numerous functionally characterized sites that are well known to be affected by EGFR signaling.[31] These included, for example, five activating tyrosine sites on the EGFR itself, the activation loop phosphosites of ERK1 and ERK2 (MAPK1 and MAPK3), activating sites on the RSK-family kinases RSK1/2 (PRKS6KA1 and 3) as well as ERK and RSK substrate sites on other kinases (Figure 2a). Furthermore, analysis of all ERK1/2 and RSK-family kinase substrate sites quantified in our dataset (55 and 11 sites, respectively) a mean increase of LFQ-MS ratios of ~2-fold, therefore confirming the EGF-dependent activation of these kinases (Figure 2b, Table S1). Because EGFR signaling does not increase the activity of PKA, we used the 34 quantified known PKA sites as a negative control, and indeed, these sites did not change in abundance (Figure 2b). All these results establish our ability to determine changes in kinase phosphorylation and activation triggered by acute signaling cues.

Kinobead/LC-MS quantifies changes in kinase complex composition

Kinobeads bind and enrich kinases through interactions with the ATP-binding pocket. However, we and others found that kinobeads enrich, along with most of the expressed kinome, hundreds of non-kinase proteins that do not bind ATP.[13, 22] Accordingly, these co-enriched proteins must be bound to kinases, suggesting that kinobead/LC-MS can analyze the composition of assembled kinase signaling complexes. Because kinase signaling complexes change in composition following kinase activation or inactivation[7-8] we reasoned that

kinobead/LC-MS can quantify these changes and that such information can be used to infer the activation state of kinases.

To test that, we applied T-test statistics to our kinobead/LC-MS protein-level dataset (15 min EGF vs. unstimulated, Table S1). Strikingly, this identified 76 proteins that significantly changed in abundance in response to EGF treatment. These included key EGFR complex components such as the adaptor proteins SHC1 and GRB2, and the ubiquitin E3 ligases CBL, CBLB and UBASH3B, which increased in abundance after EGF treatment (~10- to 45-fold increase, Figure 2c),[37] while the abundance of the EGFR itself remained nearly unchanged (1.6-fold decrease, Table S1). Because our phosphokinome profiling experiment showed that the EGFR became tyrosine phosphorylated after EGF treatment (Figure 2a), these observations indicate that kinobead/LC-MS can indeed detect activation state-dependent changes in EGFR complex composition.

To obtain additional proof for the specific co-precipitation of SHC1, GRB2, CBL and UBASH3B with the activated EGFR, we used the selective EGFR inhibitor lapatinib as a soluble competitor in kinobead pulldowns from EGF-stimulated HeLa cells (Figure 2d).[34, 38] As expected, the only kinase that was prevented to bind the kinobeads was the EGFR. In addition to EGFR, the enrichment of SHC1, GRB2, CBL, CBLB, UBASH3B and EGF was diminished by the presence of a lapatinib competitor, confirming that these proteins specifically interact with the EGFR and that kinobead/LC-MS can quantify changes in kinase complex composition.

Intrigued by these results, we mined the BioGRID protein-protein interaction database[32] for additional kinase complex components among the 76 proteins whose abundance is EGF-responsive. This revealed, for instance, decreased interactions of the Hippo kinases STK3 and LATS1 with the scaffolding proteins SAV1 and MOB1B, decreased interaction of the cell cycle kinase CDK9 with its cognate cyclin CCNT1, and increased interaction of CDK4/6 with CDKN2A (Table S1). These changes in kinase complex composition indicate inactivation of these kinases. All these observations suggest that kinobead/LC-MS has the potential to monitor the composition of a broad range of kinase complexes simultaneously, which may facilitate the highly multiplexed measurement of kinase activation states.

Kinobead/LC-MS quantifies dynamic phosphokinome changes triggered by LHCGR activation

We showed here that our kinobead/LC-MS profiling can accurately quantify phosphokinome changes in response to signaling cues. Next, we used our platform to study

steroidogenic LHCGR signaling in testicular Leydig cells.[17, 39] Knowledge of how the acute steroidogenic response is regulated by PTMs is incomplete and a system-wide study of LHCGR-triggered kinase signaling may reveal novel regulators of steroidogenesis.

To obtain a first estimate of the time course of LHCGR-mediated phosphorylation changes we quantified the activation of PKA and ERK1/2, along with the expression of the key cholesterol transporter steroidogenic acute regulatory protein StAR.[40] Accordingly, we stimulated MA10 mouse Leydig cells with 50 ng/mL luteinizing hormone (LH) for varying durations stimulated and analyzed cell lysates by western blotting. This showed that the phosphorylation of PKA substrate sites was maximal between 15-35 min and persisted until 60 min post stimulation (Figure 3a). Similarly, ERK1/2 activation loop phosphorylation was highest between 5-15 min of LH treatment and returned to basal levels 60 min after LH stimulation. In contrast, increased Star expression was detected at the 120 and 180 min timepoints, marking the apex of the acute steroidogenic response (Figure 3a). These results suggest two-stages of LHCGR signaling, i.e. a first one of continuous phosphorylation changes between early and intermediate time points (5-60 min) that is followed by a late stage of increased expression of steroidogenic proteins.

We next explored if the LHCGR activates kinases other than PKA and ERK1/2 and if activation of such kinases follows the same time course as PKA and ERK1/2 signaling. Thus, we conducted a time course experiment using our unbiased kinobead/LC-MS phosphokinome profiling platform. Using a triple-label SILAC strategy,[41] we measured phosphopeptide abundance at 0 (control), 5 and 15 min of LH treatment and at 15, 60 and 180 min of treatment (Figure 3b); this analysis quantified 1100 phosphosites on 172 kinases and 1966 sites on 803 non-kinase proteins (Table S1). To assign changes in the phosphokinome to different stages of LHCGR signaling we applied fuzzy Z-means clustering of phosphopeptide SILAC ratios,[29] identifying four clusters with distinct time profiles (Figure 3c). The first cluster described phosphosites that increase early, go through a maximum between 15 and 60 min and then drop to basal levels at 180 min. Therefore, this cluster closely followed the time course of PKA and ERK1/2 activation that we quantified by western blot analysis (Figure 3a). Reassuringly, our analysis assigned the ERK1/2 activation loop phosphorylation sites as well as 45 out of 65 highly increased PKA substrate consensus sites to this cluster (15/0 min SILAC ratio >2-fold, sites that contain the K/R-K/R-X-S/T motif, Table S1), which confirmed the accuracy of our kinobead/LC-MS time course experiment. The second cluster contained phosphorylation sites that decrease within 15 min of LH treatment and then return to basal levels at 180 min post-

stimulation, therefore indicating that the LHCGR triggers significant protein phosphatase activity at early time points. Clusters 3 and 4 described sites that continuously increase or decrease over the course of the experiment reaching their maximum/minimum at 180 min after LH stimulation. Together, these results support a two-stage model for LHCGR signaling and the acute steroidogenic response. Remarkably, analysis of kinase phosphosite SILAC ratios across the four time course clusters revealed that the phosphorylation of 69 kinases changed drastically in response to LH stimulation (164 sites with SILAC ratio >2-fold, Figure 3d). This suggests that the LHCGR utilizes a large fraction of the expressed kinome to coordinate the acute steroidogenic response. Further, our analysis revealed distinct populations of kinases that become phosphorylated or dephosphorylated at different stages of the acute steroidogenic response.

The LHCGR coordinates steroidogenesis through kinome-wide phosphorylation changes

An important goal of our study was to determine the extent and mechanism by which the LHCGR utilizes protein kinases to coordinate the acute steroidogenic response. Our SILAC time course experiments in LH-treated MA10 cells revealed that LHCGR activation affect the phosphorylation state of least 69 kinases, and that the majority of phosphokinome changes undergo a maximum within 15-60 min after stimulation (clusters 1 and 2, Figure 3c and 3d**,** Table S1), indicating that early phosphorylation events play a key role in the acute steroidogenic response. Accordingly, we moved on to obtain a more comprehensive picture of early (15 min) LHCGR-dependent phosphoproteome changes and the pathways they affect. To this end, we conducted both an LFQ-MS kinobead/LC-MS phosphokinome analysis and a global phosphoproteomics analysis in MA10 cells comparing 15 min LH treatment with basal control cells (50 ng/mL LH, 5 biological replicates/condition). Combined, these analyses quantified 1485 phosphosites on 252 kinases and 10625 sites on 2619 non-kinase substrate proteins (Table S1). Compared to our SILAC analysis, these experiments quantified ~1.5-times more phosphosites on kinases and ~5-times more sites on non-kinase substrates.

To explore which cellular pathways are affected by LHCGR signaling, we first analyzed our LFQ global phosphoproteome and kinobead/LC-MS phosphokinome datasets for LH-dependent changes in phosphosites and proteins abundance. T-test analysis revealed that 217 sites on 106 kinases and 1218 sites on 700 non-kinase proteins significantly changed after 15 min of LH treatment. An additional 48 proteins changed in abundance in our kinobead/LC-MS protein-level data (Figure 4a and Table S1). Among these proteins, we identified the PKA catalytic subunits α and β (Prkaca and Prkacb) and regulatory subunits 1α and 1β (Prkar1a and

Prkar1b), the calcium/calmodulin-dependent kinase Camk2d, and the salt-inducible kinase 3 (Sik3). Because abundance changes of these kinases and other kinase interactors indicate altered kinase activity, we integrated the protein abundance data in our pathway analysis. We then used STRING[42] to perform a gene ontology – biological process (GOBP) term enrichment analysis (Figure 4b and Table S1). Analyzing both enrichment of GOBP terms by proteins that significantly change in phosphorylation/abundance and those that do not we eliminated biases introduced by quantification of a limited subset of the entire MA10 cell proteome. Strikingly, GOBP term analysis revealed strong enrichment of terms associated endocytosis, vesicle transport, mitochondrion and ER function, and cytoskeleton dynamics (Figure 4b). Vesicle transport and mitochondrion/ER function are tightly linked to cholesterol availability through its uptake, mobilization and cellular transport to the organelles where steroid precursors are metabolized.[19-20] Cytoskeleton components act as scaffolds for vesicular transport, ER/mitochondria function and positioning and disruption of these components can inhibit steroid biosynthesis.[19] These results strongly suggest that many early LH-triggered phosphorylation changes regulate cholesterol availability. In addition, we identify GOBP terms related to other, basic cellular processes enriched among phospho-regulated proteins, including regulation of the mitotic cell cycle, cell death, differentiation and, most prominently, signaling by stress-activated MAPKs (Figure 4b). We hypothesize that the LHCGR regulates these pathways to ensure cellular homeostasis while facing cellular stress caused by a rapid and massive increase in steroid biosynthesis.

Kinases that regulate early events in the acute steroidogenic response

Our collated phosphokinome, global phosphoproteome and kinobead protein abundance data revealed that 40% of the MA10 cell kinome undergoes regulation in the early stages of the acute steroidogenic response (Table S1). Next, we classified and prioritized kinases to identify those that are likely to have functional roles in specific aspects of LHCGR signaling, i.e. cholesterol availability and metabolism as well as crosstalk with the cell cycle, stress-activated MAPK and apoptosis signaling, and cell differentiation pathways (Figure 4b). To this end, we first determined kinase association with LH-sensitive signaling pathways. Mining of our STRING GOBP-term enrichment dataset revealed that 37 of 106 LH-sensitive kinases regulate cytoskeleton dynamics (Group A, Figure 4b and Table S1) , vesicle transport and endocytosis, and ER/mitochondrial functions (Figure 4c). Furthermore, 36 of 106 kinases were associated with regulation of the cell cycle, cell death, differentiation and stress activated MAPK signaling (Group B, Figure 4c), and residual kinases could not be assigned to any of the GOBP gene sets

(Group C, Figure 4c). As the main criteria for prioritization we used the magnitude of LFQ-MS ratios, assuming that higher ratios indicate greater biological significance, and the presence of LH-responsive sites that have a known role in kinase regulation.[31]

Accordingly, we found that Group A included 14 kinases that are linked to vesicular trafficking, indicating the importance of this process for steroidogenesis. Among these kinases, cyclin G-associated kinase (Gak), cyclin-dependent kinase 16 (Cdk16), and SCY1-like protein 2 (Scyl2) showed the most dramatic changes in phosphorylation (mean absolute LFQ-MS ratios of ~5-fold to ~60-fold, Figure 4c). Notably, none of these kinases has known roles in steroidogenesis. Increased phosphorylation of Cdk16 (S153) indicated deactivation of the kinase, whereas LH-responsive sites on Gak and Scyl2 have not been characterized yet.[31] Gak and Scyl2 localize to the trans-Golgi network (TNG; both kinases) and lysosomes (Scyl2), where they regulate clathrin-mediated vesicle trafficking. Because the TNG is a hub for relocating cholesterol from lysosomes to target organelles,[20, 43-44] these two kinases may have important and unexplored roles in cholesterol trafficking and steroidogenesis. The other 28 kinases in Group A are linked to cytoskeleton dynamics (Figure 4c). Hence, several highly LH-sensitive kinases (LFQ-MS ratio of ~4 to ~6) regulate microtubule polymerization, for instance the STE20-like kinase Slk and the MAP/microtubule affinity-regulating kinases 2 and 4 (Mark2 and 4), or actin and stress fiber assembly, for example the Rho-associated kinase Rock2, the cytoplasmic tyrosine kinases Abl2 and Fer, and the LIM domain kinase 1 (Limk1). Of these kinases only Rock2 has been associated with steroidogenesis previously.[45] Remarkably, our analyses identified that four cytoskeleton-associated kinases likely become activated following LH treatment, i.e. Slk (decreased S347), Mark2 (decreased T593), Fer (increased Y715) and Abl2 (increased Y439)[31] – these kinases are prime candidates for regulating cytoskeleton-dependent steroidogenic processes.[19]

LH-induced phosphorylation changes in Group B kinases indicated activation of Map3k2 (increased S153) and Tao kinase 3 (Taok3, increased S324), which can lead to p38α activation; the latter is required for efficient steroidogenesis.[46] In addition, activation of RSK1 and 2 (Rps6ka1 and 3) and downstream phosphorylation of the ephrin receptor Epha2 (S898) indicated increased survival signaling. Interestingly, Group B included 24 kinases that regulate cell death and cellular stress signaling, suggesting that these processes are important for LHCGR signaling and steroidogenesis (Figure 4c). Most LH-responsive phosphosites on these kinases have no known function. however, our finding that survival kinases become activated

suggests that proapoptotic kinases such as the Hippo kinase Stk3, and the death receptor-associated kinases Ripk1 and Ripk2 may become inactivated.

Group C kinases could not be assigned to any of the LH-responsive GOBP gene sets (Figure 4b and 4c). However, this group contained several kinases known to play key roles in steroidogenesis, for instance calcium/calmodulin-dependent kinases (Camk2a-d),[47] the PKA catalytic subunits, the salt inducible kinases 2 and 3 (Sik2 and 3),[48] and kinases associated with proliferation (BRAF, FGFR4, and others). In addition, other highly phospho-regulated kinases in Group C have been reported to play a role in cytoskeleton-associated processes, but have not been linked to the corresponding GOBP term yet; examples are the never in mitosis A-related kinase Nek3, the myosin light chain kinase (Mylk), and the microtubule-associated kinases Mast2-4 (Figure 4c). This shows that not all LHCGR signaling pathways can be determined by GOBP term enrichment analysis and, more importantly, that our dataset can be mined to identify additional, unchartered LH-responsive pathways (Figure 4a and Table S1)

Finally, we asked if PKA, the steroidogenic master regulator,[18] is involved in crosstalk with the 106 other LH-responsive kinases. Accordingly, we searched amino acid sequences flanking phosphosites on regulated kinases for the presence of the PKA substrate consensus sequence (K/R-K/R-X-S/T). Strikingly, 29 of the 106 LH-sensitive kinases had phosphosites matching this consensus sequence (Figure 4c), yet only 10 of these sites were previously reported to be PKA substrates.[31] Hence, our data significantly expands the number of PKA-regulated kinases and demonstrates that the LHCGR controls a substantial fraction of the regulated kinome through its main effector kinase PKA.

Discussion:

In the first part of our study, we introduced a facile kinobead/LC-MS workflow for rapid and deep profiling of the kinome and phosphokinome. Our previous studies demonstrated that the sensitivity of kinobead/LC-MS can be drastically improved by replacing in-gel cleanup and digestion of kinase-enriched samples with one simple on-bead preparation step.[21-22, 34] This improved sensitivity allowed us to profile the kinome-wide selectivity and affinity of entire kinase inhibitor libraries, and the expression levels of ~200-250 native kinases in single LC-MS runs.[49] We showed here that our next generation protocol for on-bead sample preparation causes another leap in sensitivity. Most importantly, we introduced a phosphopeptide enrichment step into our kinobead/LC-MS workflow, which now enables phosphokinome analyses with unprecedented sensitivity. Thus, our kinome profiling platform can quantify the kinome to a

depth of ~200-250 kinases and ~800-1000 kinase phosphorylation sites in a single kinobead/LC-MS experiment using just 1 mg of protein sample. The reduced protein requirement allows simple and rapid sample preparation and, therefore, facilitates the comparison of multiple conditions and model systems with greatly increased throughput. We believe that the increased sensitivity and throughput of our approach will enable routine use of kinobead/LC-MS kinome profiling in cell lines and animal models. The large sample requirements for kinobead/LC-MS phosphokinome profiling prevented the analysis of tissue samples such as tumor biopsies. We expect that our approach will facilitate the analysis of clinical tissue specimens to determine kinome activity with unprecedented sensitivity.

Protein kinases drive adverse cancers phenotypes such as uncontrolled proliferation, increased survival and metastasis and thus became important drug targets.[3, 50-51] Accordingly, knowledge of aberrant kinase activities may be used as predictive biomarker for targeted chemotherapy[52]. We believe that our approach can be applied for biomarker discovery in clinical proteomics and personalized oncology. System-wide unbiased measurements of kinase activity in tumor samples can not only quantify the activity of well-studied oncogenic driver kinases but also identify novel oncogenic kinases that may serve as drug targets. Importantly, we showed here for the first time that kinobead/LC-MS can detect dynamic changes in kinase complex composition and that these changes can specify the activation state of kinases. This unique property of kinobead/LC-MS will greatly enhance its utility for kinome activity profiling in cell signal transduction research and clinical proteomics. We envision that improved protocols that favor the co-purification of kinase-regulatory proteins will facilitate comprehensive, system-wide measurements of kinase complex dynamics.[13]

In the second part of our study, we used our kinobead/LC-MS profiling approach to quantify dynamic changes in kinome activity downstream of the LHCGR, a GPCR that controls steroid biosynthesis in testicular Leydig cells.[15] Our analyses revealed that LHCGR activation affected the phosphorylation state of at least 106 protein kinases, i.e. 40% of the detected MA10 cell kinome. Previous reports have shown that multiple kinase-dependent pathways act in concert to facilitate steroid biosynthesis through the transcriptional and post-translational control of steroidogenic factors such as the steroid acute-regulatory protein STAR (STARD1) and the hormone-sensitive lipase (LIPE).[18] Our study suggests that the LHCGR and PKA utilize many other kinase-dependent pathways that control cytoskeleton dynamics, vesicle trafficking and endocytosis to coordinate cholesterol availability, and that these regulatory events occur very early during the acute steroidogenic response. We show that LHCGR signaling also affects

other, basic cellular processes such as apoptotic signaling, cell differentiation, the cell cycle and proliferation. Evidence from our phosphoproteome dataset indicates that transport processes and survival signaling are activated in response to LH, while apoptosis, cell cycle and proliferation signaling are suppressed. We speculate that this crosstalk of LHCGR-PKA signaling with other diverse pathways is necessary to synchronize cholesterol availability with the transcription of steroidogenic proteins, the activation of metabolic enzymes and other vital cellular processes. This may allow steroid biosynthesis to occur in a timely manner after hormone stimulation while halting the cell cycle and suppressing cellular stress responses. In conclusion, our results uncover the regulation of the kinome in multiple signaling pathways downstream of the LHCGR and greatly expand the current knowledge of post-translational control of steroid biosynthesis and Gαs-coupled GPCR signaling; our dataset is an important resource enabling focused studies of the molecular mechanisms in these signaling systems.

Associated Content:

Supporting Information

Supplemental Table S1 containing data of protein and phosphopeptide quantification from all the MA10 SILAC, MA10 LFQ-MS and HeLa LFQ-MS experiments (MaxQuant search engine output). Table S1 also contains the results from M-fuzz time course clustering and the STRING GOBP term enrichment analysis.

Author Information:

Corresponding Authors

*Correspondence: shaoen@u.washington.edu (S-E.O.), golkom@uw.edu (M.G.)

Notes

The authors declare no competing financial interest.

Acknowledgements

We thank John D Scott, Anthony K. Leung, David Shechner, and members of the Ong and Maly Labs for comments on the manuscript. This work was supported by grants from the National Institutes of Health issued under the award numbers R01GM086858, R01GM129090, R01AR065459, R21EB018384, R21CA177402, K22CA201229-01, by the Sidney Kimmel Foundation and by a postdoctoral research fellowship of the German Research Foundation (DFG) awarded to M.G. (GO 2358/1-1). We gratefully acknowledge funding from the

Department of Defense under the award number CA150370 as well as the Fibrolamellar Cancer Foundation. The content is solely the responsibility of the authors and does not necessarily represent the official views of the National Institutes of Health.

References:

1. Manning, G.; Whyte, D. B.; Martinez, R.; Hunter, T.; Sudarsanam, S., The protein kinase complement of the human genome. *Science* **2002,** *298* (5600), 1912-34.
2. Fleuren, E. D.; Zhang, L.; Wu, J.; Daly, R. J., The kinome 'at large' in cancer. *Nat Rev Cancer* **2016,** *16* (2), 83-98.
3. Ferguson, F. M.; Gray, N. S., Kinase inhibitors: the road ahead. *Nat Rev Drug Discov* **2018,** *17* (5), 353-377.
4. Venne, A. S.; Kollipara, L.; Zahedi, R. P., The next level of complexity: crosstalk of posttranslational modifications. *Proteomics* **2014,** *14* (4-5), 513-24.
5. Vu, L. D.; Gevaert, K.; De Smet, I., Protein Language: Post-Translational Modifications Talking to Each Other. *Trends Plant Sci* **2018,** *23* (12), 1068-1080.
6. Choudhary, C.; Mann, M., Decoding signalling networks by mass spectrometry-based proteomics. *Nat Rev Mol Cell Biol* **2010,** *11* (6), 427-39.
7. Nolen, B.; Taylor, S.; Ghosh, G., Regulation of protein kinases; controlling activity through activation segment conformation. *Molecular cell* **2004,** *15* (5), 661-75.
8. Endicott, J. A.; Noble, M. E.; Johnson, L. N., The structural basis for control of eukaryotic protein kinases. *Annu Rev Biochem* **2012,** *81*, 587-613.
9. Daub, H.; Olsen, J. V.; Bairlein, M.; Gnad, F.; Oppermann, F. S.; Korner, R.; Greff, Z.; Keri, G.; Stemmann, O.; Mann, M., Kinase-selective enrichment enables quantitative phosphoproteomics of the kinome across the cell cycle. *Molecular cell* **2008,** *31* (3), 438-48.
10. Bantscheff, M.; Eberhard, D.; Abraham, Y.; Bastuck, S.; Boesche, M.; Hobson, S.; Mathieson, T.; Perrin, J.; Raida, M.; Rau, C.; Reader, V.; Sweetman, G.; Bauer, A.; Bouwmeester, T.; Hopf, C.; Kruse, U.; Neubauer, G.; Ramsden, N.; Rick, J.; Kuster, B.; Drewes, G., Quantitative chemical proteomics reveals mechanisms of action of clinical ABL kinase inhibitors. *Nat Biotechnol* **2007,** *25* (9), 1035-44.
11. Dulla, K.; Daub, H.; Hornberger, R.; Nigg, E. A.; Korner, R., Quantitative site-specific phosphorylation dynamics of human protein kinases during mitotic progression. *Mol Cell Proteomics* **2010,** *9* (6), 1167-81.
12. Schreiber, T. B.; Mausbacher, N.; Keri, G.; Cox, J.; Daub, H., An integrated phosphoproteomics work flow reveals extensive network regulation in early lysophosphatidic acid signaling. *Mol Cell Proteomics* **2010,** *9* (6), 1047-62.
13. Sharma, K.; Kumar, C.; Keri, G.; Breitkopf, S. B.; Oppermann, F. S.; Daub, H., Quantitative analysis of kinase-proximal signaling in lipopolysaccharide-induced innate immune response. *Journal of proteome research* **2010,** *9* (5), 2539-49.
14. Oppermann, F. S.; Gnad, F.; Olsen, J. V.; Hornberger, R.; Greff, Z.; Keri, G.; Mann, M.; Daub, H., Large-scale proteomics analysis of the human kinome. *Molecular & cellular proteomics : MCP* **2009,** *8* (7), 1751-64.
15. Ascoli, M.; Fanelli, F.; Segaloff, D. L., The lutropin/choriogonadotropin receptor, a 2002 perspective. *Endocr Rev* **2002,** *23* (2), 141-74.
16. Miller, W. L.; Auchus, R. J., The molecular biology, biochemistry, and physiology of human steroidogenesis and its disorders. *Endocr Rev* **2011,** *32* (1), 81-151.

17. Golkowski, M.; Shimizu-Albergine, M.; Suh, H. W.; Beavo, J. A.; Ong, S. E., Studying mechanisms of cAMP and cyclic nucleotide phosphodiesterase signaling in Leydig cell function with phosphoproteomics. *Cell Signal* **2016,** *28* (7), 764-78.
18. Stocco, D. M.; Wang, X.; Jo, Y.; Manna, P. R., Multiple signaling pathways regulating steroidogenesis and steroidogenic acute regulatory protein expression: more complicated than we thought. *Mol Endocrinol* **2005,** *19* (11), 2647-59.
19. Sewer, M. B.; Li, D., Regulation of steroid hormone biosynthesis by the cytoskeleton. *Lipids* **2008,** *43* (12), 1109-15.
20. Hu, J.; Zhang, Z.; Shen, W. J.; Azhar, S., Cellular cholesterol delivery, intracellular processing and utilization for biosynthesis of steroid hormones. *Nutr Metab (Lond)* **2010,** *7*, 47.
21. Golkowski, M.; Brigham, J. L.; Perera, G. K.; Romano, G. E.; Maly, D. J.; Ong, S. E., Rapid profiling of protein kinase inhibitors by quantitative proteomics. *MedChemComm* **2014,** *5* (3), 363-369.
22. Golkowski, M.; Vidadala, R. S.; Lombard, C. K.; Suh, H. W.; Maly, D. J.; Ong, S. E., Kinobead and Single-Shot LC-MS Profiling Identifies Selective PKD Inhibitors. *Journal of proteome research* **2017,** *16* (3), 1216-1227.
23. Wang, H.; Qian, W. J.; Mottaz, H. M.; Clauss, T. R.; Anderson, D. J.; Moore, R. J.; Camp, D. G., 2nd; Khan, A. H.; Sforza, D. M.; Pallavicini, M.; Smith, D. J.; Smith, R. D., Development and evaluation of a micro- and nanoscale proteomic sample preparation method. *Journal of proteome research* **2005,** *4* (6), 2397-403.
24. Rappsilber, J.; Mann, M.; Ishihama, Y., Protocol for micro-purification, enrichment, pre-fractionation and storage of peptides for proteomics using StageTips. *Nature protocols* **2007,** *2* (8), 1896-906.
25. Jersie-Christensen, R. R.; Sultan, A.; Olsen, J. V., Simple and Reproducible Sample Preparation for Single-Shot Phosphoproteomics with High Sensitivity. *Methods Mol Biol* **2016,** *1355*, 251-60.
26. Villen, J.; Gygi, S. P., The SCX/IMAC enrichment approach for global phosphorylation analysis by mass spectrometry. *Nature protocols* **2008,** *3* (10), 1630-8.
27. Ficarro, S. B.; Adelmant, G.; Tomar, M. N.; Zhang, Y.; Cheng, V. J.; Marto, J. A., Magnetic bead processor for rapid evaluation and optimization of parameters for phosphopeptide enrichment. *Analytical chemistry* **2009,** *81* (11), 4566-75.
28. Tyanova, S.; Temu, T.; Sinitcyn, P.; Carlson, A.; Hein, M. Y.; Geiger, T.; Mann, M.; Cox, J., The Perseus computational platform for comprehensive analysis of (prote)omics data. *Nat Methods* **2016,** *13* (9), 731-40.
29. Kumar, L.; M, E. F., Mfuzz: a software package for soft clustering of microarray data. *Bioinformation* **2007,** *2* (1), 5-7.
30. Szklarczyk, D.; Gable, A. L.; Lyon, D.; Junge, A.; Wyder, S.; Huerta-Cepas, J.; Simonovic, M.; Doncheva, N. T.; Morris, J. H.; Bork, P.; Jensen, L. J.; Mering, C. V., STRING v11: protein-protein association networks with increased coverage, supporting functional discovery in genome-wide experimental datasets. *Nucleic acids research* **2019,** *47* (D1), D607-D613.
31. Hornbeck, P. V.; Zhang, B.; Murray, B.; Kornhauser, J. M.; Latham, V.; Skrzypek, E., PhosphoSitePlus, 2014: mutations, PTMs and recalibrations. *Nucleic acids research* **2015,** *43* (Database issue), D512-20.
32. Chatr-Aryamontri, A.; Oughtred, R.; Boucher, L.; Rust, J.; Chang, C.; Kolas, N. K.; O'Donnell, L.; Oster, S.; Theesfeld, C.; Sellam, A.; Stark, C.; Breitkreutz, B. J.; Dolinski, K.; Tyers, M., The BioGRID interaction database: 2017 update. *Nucleic acids research* **2017,** *45* (D1), D369-D379.
33. Feist, P.; Hummon, A. B., Proteomic challenges: sample preparation techniques for microgram-quantity protein analysis from biological samples. *Int J Mol Sci* **2015,** *16* (2), 3537-63.
34. Golkowski, M.; Maly, D. J.; Ong, S. E., Proteomic Profiling of Protein Kinase Inhibitor Targets by Mass Spectrometry. *Methods Mol Biol* **2017,** *1636*, 105-117.

35. Olsen, J. V.; Blagoev, B.; Gnad, F.; Macek, B.; Kumar, C.; Mortensen, P.; Mann, M., Global, in vivo, and site-specific phosphorylation dynamics in signaling networks. *Cell* **2006,** *127* (3), 635-48.
36. Sharma, K.; D'Souza, R. C.; Tyanova, S.; Schaab, C.; Wisniewski, J. R.; Cox, J.; Mann, M., Ultradeep human phosphoproteome reveals a distinct regulatory nature of Tyr and Ser/Thr-based signaling. *Cell reports* **2014,** *8* (5), 1583-94.
37. Schulze, W. X.; Deng, L.; Mann, M., Phosphotyrosine interactome of the ErbB-receptor kinase family. *Mol Syst Biol* **2005,** *1*, 2005 0008.
38. Ong, S. E.; Schenone, M.; Margolin, A. A.; Li, X.; Do, K.; Doud, M. K.; Mani, D. R.; Kuai, L.; Wang, X.; Wood, J. L.; Tolliday, N. J.; Koehler, A. N.; Marcaurelle, L. A.; Golub, T. R.; Gould, R. J.; Schreiber, S. L.; Carr, S. A., Identifying the proteins to which small-molecule probes and drugs bind in cells. *Proc Natl Acad Sci U S A* **2009,** *106* (12), 4617-22.
39. Shimizu-Albergine, M.; Van Yserloo, B.; Golkowski, M. G.; Ong, S. E.; Beavo, J. A.; Bornfeldt, K. E., SCAP/SREBP pathway is required for the full steroidogenic response to cyclic AMP. *Proc Natl Acad Sci U S A* **2016,** *113* (38), E5685-93.
40. Miller, W. L., Steroidogenic acute regulatory protein (StAR), a novel mitochondrial cholesterol transporter. *Biochim Biophys Acta* **2007,** *1771* (6), 663-76.
41. Ong, S. E.; Mann, M., Mass spectrometry-based proteomics turns quantitative. *Nat Chem Biol* **2005,** *1* (5), 252-62.
42. Szklarczyk, D.; Franceschini, A.; Wyder, S.; Forslund, K.; Heller, D.; Huerta-Cepas, J.; Simonovic, M.; Roth, A.; Santos, A.; Tsafou, K. P.; Kuhn, M.; Bork, P.; Jensen, L. J.; von Mering, C., STRING v10: protein-protein interaction networks, integrated over the tree of life. *Nucleic acids research* **2015,** *43* (Database issue), D447-52.
43. Hao, M.; Lin, S. X.; Karylowski, O. J.; Wustner, D.; McGraw, T. E.; Maxfield, F. R., Vesicular and non-vesicular sterol transport in living cells. The endocytic recycling compartment is a major sterol storage organelle. *J Biol Chem* **2002,** *277* (1), 609-17.
44. Luo, J.; Jiang, L. Y.; Yang, H.; Song, B. L., Intracellular Cholesterol Transport by Sterol Transfer Proteins at Membrane Contact Sites. *Trends Biochem Sci* **2019,** *44* (3), 273-292.
45. Otis, M.; Gallo-Payet, N., Differential involvement of cytoskeleton and rho-guanosine 5'-triphosphatases in growth-promoting effects of angiotensin II in rat adrenal glomerulosa cells. *Endocrinology* **2006,** *147* (11), 5460-9.
46. Zaidi, S. K.; Shen, W. J.; Bittner, S.; Bittner, A.; McLean, M. P.; Han, J.; Davis, R. J.; Kraemer, F. B.; Azhar, S., p38 MAPK regulates steroidogenesis through transcriptional repression of STAR gene. *J Mol Endocrinol* **2014,** *53* (1), 1-16.
47. Abdou, H. S.; Villeneuve, G.; Tremblay, J. J., The calcium signaling pathway regulates leydig cell steroidogenesis through a transcriptional cascade involving the nuclear receptor NR4A1 and the steroidogenic acute regulatory protein. *Endocrinology* **2013,** *154* (1), 511-20.
48. Katoh, Y.; Takemori, H.; Horike, N.; Doi, J.; Muraoka, M.; Min, L.; Okamoto, M., Salt-inducible kinase (SIK) isoforms: their involvement in steroidogenesis and adipogenesis. *Mol Cell Endocrinol* **2004,** *217* (1-2), 109-12.
49. Golkowski, M.; Perera, G. K.; Vidadala, V. N.; Ojo, K. K.; Van Voorhis, W. C.; Maly, D. J.; Ong, S. E., Kinome chemoproteomics characterization of pyrrolo[3,4-c]pyrazoles as potent and selective inhibitors of glycogen synthase kinase 3. *Mol Omics* **2018,** *14* (1), 26-36.
50. Shibue, T.; Weinberg, R. A., EMT, CSCs, and drug resistance: the mechanistic link and clinical implications. *Nat Rev Clin Oncol* **2017,** *14* (10), 611-629.
51. Cohen, P.; Alessi, D. R., Kinase drug discovery--what's next in the field? *ACS Chem Biol* **2013,** *8* (1), 96-104.
52. Quan, C.; Xiao, J.; Liu, L.; Duan, Q.; Yuan, P.; Zhu, F., Protein Kinases as Tumor Biomarkers and Therapeutic Targets. *Curr Pharm Des* **2017,** *23* (29), 4209-4225.

Figures 1-4:

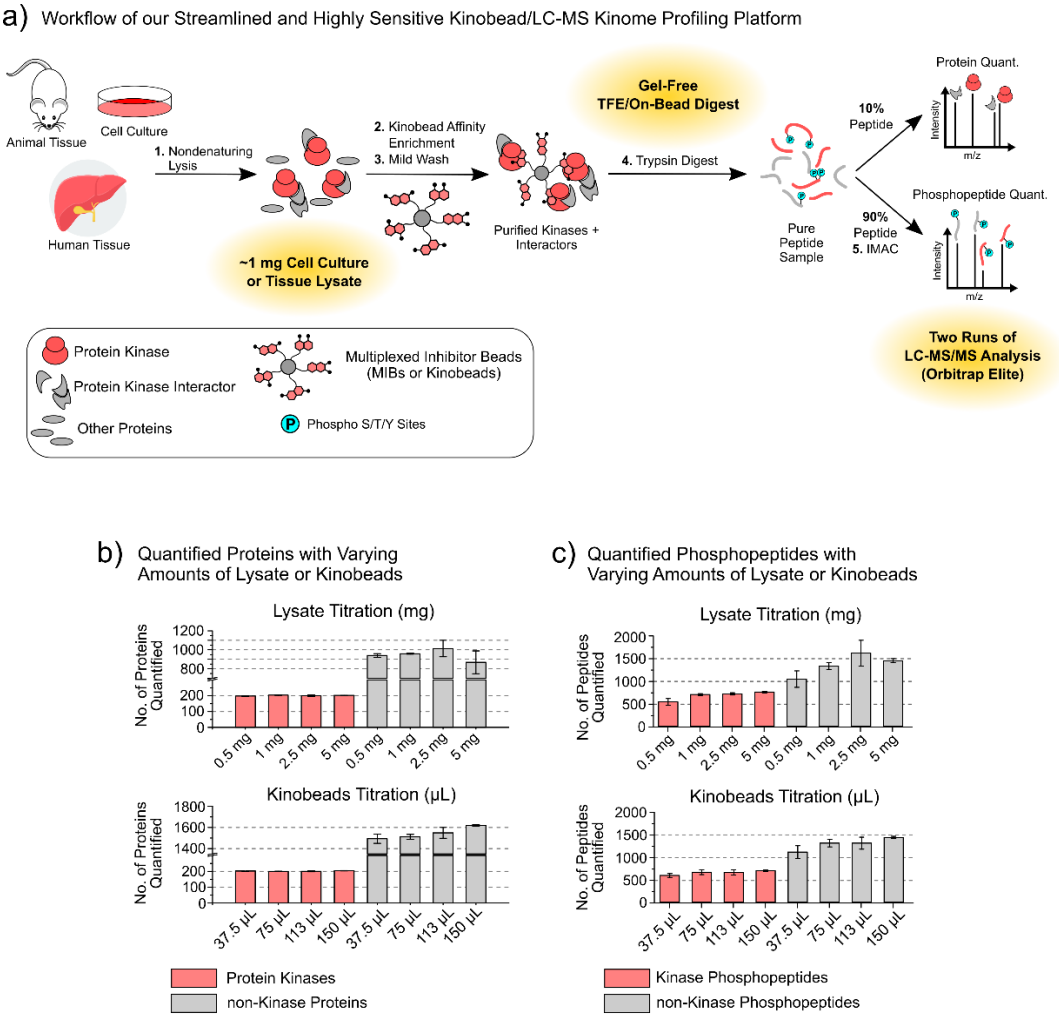

Figure 1. Comprehensive kinome profiling with kinobead/LC-MS.

(**a**) Workflow of our kinobead/LC-MS analytical platform.

(**b**) Kinobead/LC-MS quantification of proteins (kinases and non-kinases) in HeLa cell lysate using varying amounts of protein sample and 100 µL kinobeads or varying amounts of kinobeads and 1 mg protein sample. Bars represent the mean of three biological replicates, error bars are the S.D. Data were obtained in single analytical LC-MS runs on a Thermo Scientific Orbitrap Elite mass spectrometer.

(**c**) Same as in (b) but phosphopeptides derived from protein kinases and co-enriched non-kinase proteins.

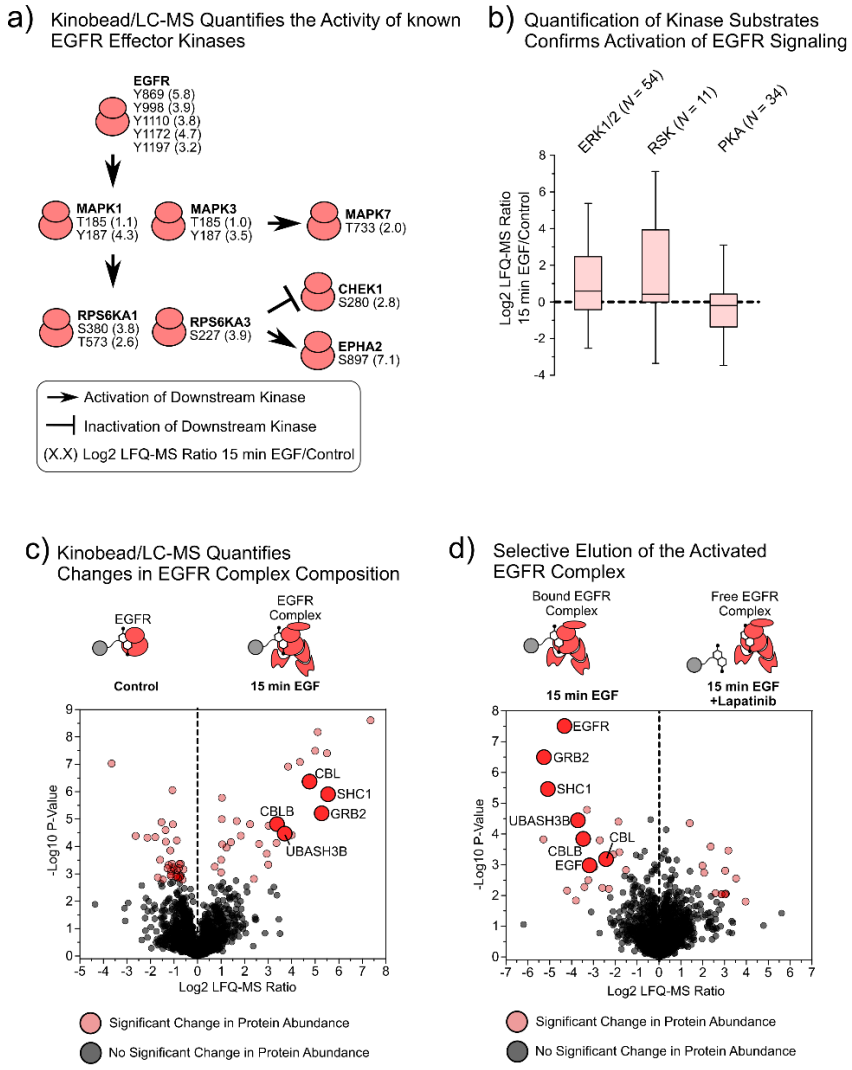

Figure 2. Kinobead/LC-MS analysis of the EGFR signaling pathway model.

(**a**) Flow diagram of known EGFR effector kinases in HeLa cells quantified by kinobead/LC-MS phosphokinome analysis. Activating/inactivating phosphorylation sites that change in response to 15 min EGF treatment are shown.

(**b**) Log2 LFQ-MS ratios of known ERK1/2, RSK-family kinase (RPS6KA1-3), and PKA substrate sites (PhosphoSite Plus database)[31] in response to 15 min EGF stimulation. A shift in ratios of ERK1/2 and RSK kinase substrate sites indicates activation of these kinases, whereas PKA substrates did not change (negative control).

(**c**) Treatment of HeLa cells with EGF (50 ng/mL, 15 min) leads to protein abundance changes as was measured by LFQ kinobead/LC-MS profiling. Result of a two-sample T-Test with BH correction (FDR = 0.05, 5 replicates/condition)

(**d**) Selective competition of EGFR signaling complexes. Comparison of HeLa cells treated with 50 ng/mL EGF for 15 min with HeLa cells treated in the same manner but 10 µM of the selective EGFR inhibitor lapatinib spiked into the cell lysate prior to kinobead affinity enrichment (see also (**c**)).

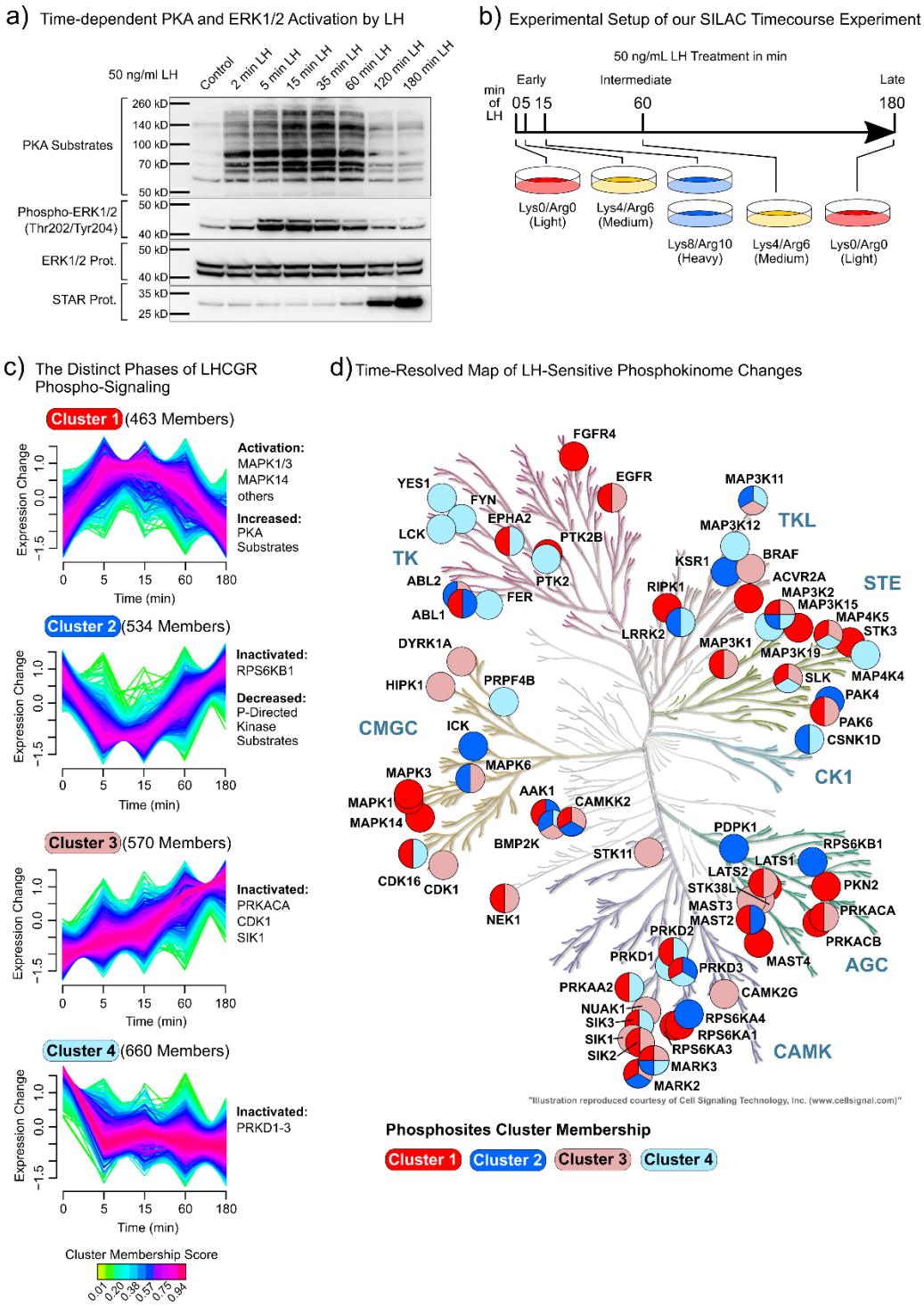

Figure 3. Dynamic phosphokinome changes triggered by LHCGR activation.

(**a**) Western blot analysis of MA10 cells treated with 50 ng/mL LH over a time course of 3 h.

(**b**) Experimental design of our triplex SILAC kinobead/LC-MS time course experiment in LH-stimulated MA10 cells.

(**c**) Fuzzy C-means clustering of phosphopeptide intensities measured following LH-stimulation in MA10 cells for 0, 5, 15, 60 and 180 min (see also (b)).

(**d**) Overlay of kinases that change in phosphorylation state in response to LH-treatment with the human kinome dendrogram. Kinases are color coded according to the time course cluster membership of their phosphosites (see (**c**)).

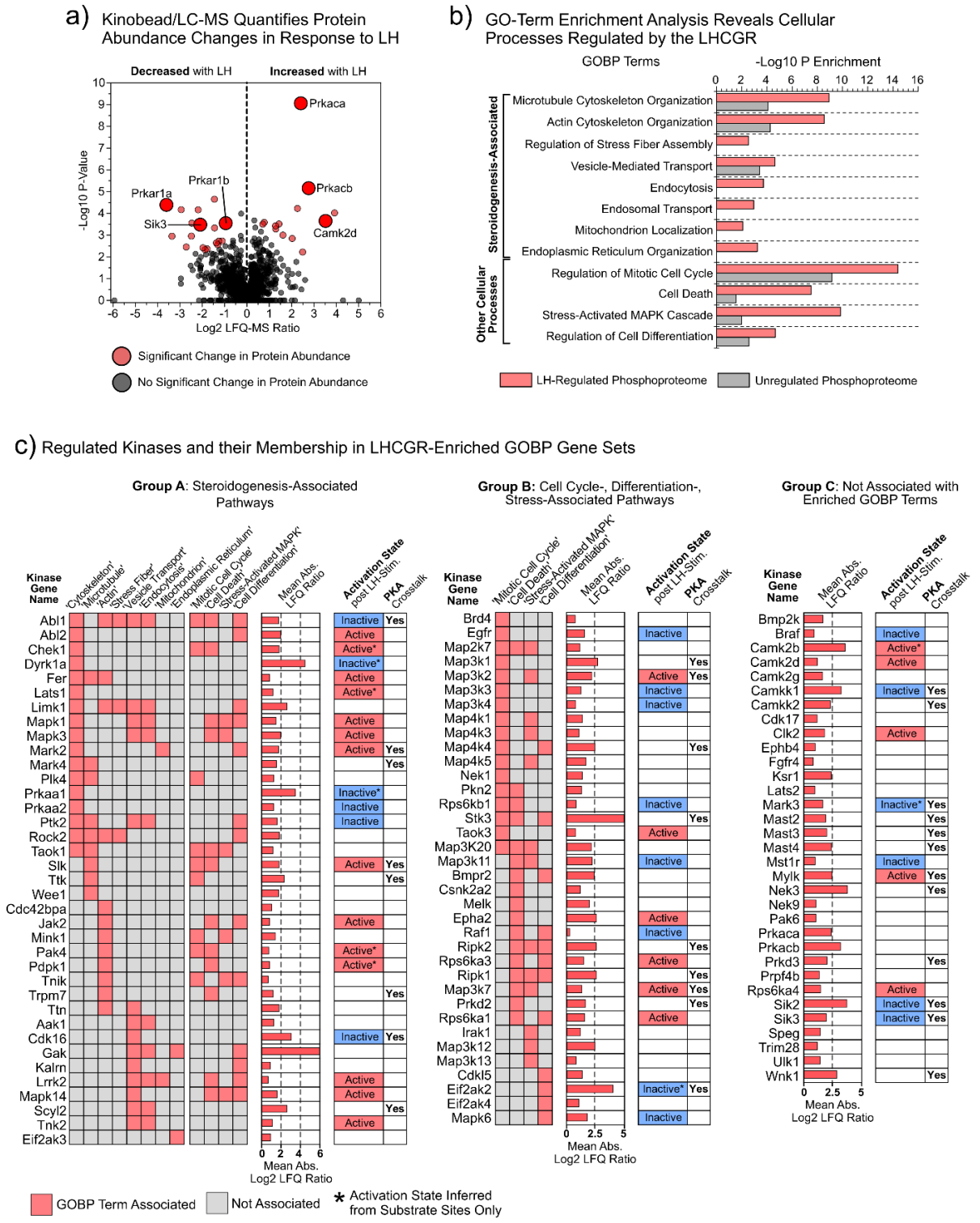

Figure 4. Protein kinases that change in phosphorylation during the early stage of steroidogenesis.

(**a**) Acute treatment of MA10 cells with LH (50 ng/mL, 15 min) leads to protein abundance changes as was measured by LFQ kinobead/LC-MS profiling. Result of a two-sample T-Test with BH correction (FDR = 0.05, 5 replicates/condition)

(**b**) STRING analysis of GOBP terms enriched among proteins that change in phosphorylation in response to 15 min LH treatment and among proteins that do not change in phosphorylation (control, see Table S1).[42]

(**c**) LHCGR-regulated kinases associated with GOBP terms relevant for steroid biosynthesis and cholesterol transport (Group A, left panel), relevant for cell cycle, cell death and differentiation (Group B, middle panel) and kinases that are not included in the enriched GOBP terms enriched (see (**b**), Group C, right panel). Changes in activation state after 15 min LH treatment and the presence of PKA consensus sequence sites (K/R-K/R-XS/T motif) are also shown.